

# Radiation-induced order–disorder transition in $p^+ - n$ InGaP solar cells

M. J. Romero,<sup>a)</sup> D. Araújo, and R. García

*Departamento de Ciencia de los Materiales e I.M. y Q.I., Facultad de Ciencias, Universidad de Cádiz, E-11510, Puerto Real (Cádiz), Spain*

R. J. Walters and G. P. Summers

*Naval Research Laboratory, Code 6615, 4555 Overlook Avenue, S.W., Washington, DC 20375*

S. R. Messenger

*SFA Inc., Largo, Maryland 20744*

(Received 10 November 1998; accepted for publication 25 February 1999)

The effects of electron and proton irradiation on  $p^+ - n$  InGaP solar cells grown on GaAs substrates are investigated using cathodoluminescence (CL) and transmission electron microscopy (TEM). The CL measurements confirm the higher radiation resistance and defect annealing properties of InGaP compared to those of GaAs. The CL measurements also indicate the occurrence of a radiation-induced sublattice order–disorder transition in InGaP. TEM reveals the presence of ordering domains in the as-grown cells, which are effectively removed by radiation-induced defects. The results should be useful in the fabrication of radiation-resistant single-junction and dual-junction InGaP solar cells for space. © 1999 American Institute of Physics. [S0003-6951(99)01517-X]

Monolithic multijunction solar cells have been shown to have much higher efficiencies than single-junction cells due to their larger range of spectral sensitivity. The main technical challenge in the growth of these cells is to lattice match the different materials at their interfaces to prevent the production of threading dislocations. For space applications there is the added requirement of radiation tolerance. Under irradiation with high-energy electrons or protons, as suffered in space, all junctions are degraded simultaneously. Since they are connected in series, the most vulnerable junction determines the radiation response of the whole cell.

The highest efficiency commercially available space solar cell is currently the dual-junction InGaP<sub>2</sub>/GaAs cell grown by organometallic vapor phase epitaxy (OMVPE) on a Ge substrate. Laboratory prototypes of this technology have been made with record efficiencies.<sup>1</sup> In this letter, we report cathodoluminescence (CL) and transmission electron microscopy (TEM) measurements made on single-junction (SJ)  $p^+ - n$  InGaP cells grown on GaAs substrates. It is shown that InGaP grown on GaAs by OMVPE initially consists of ordered sublattice domains. However, after irradiation with high-energy electrons or protons, displacement damage defects remove the sublattice ordering in the as-grown InGaP in a manner that could be related to an order–disorder transition. The results also confirm the better radiation tolerance of InGaP as compared to GaAs.

Details of the cells, grown by OMVPE at the Research Triangle Institute, are given in Table I. Three solar cells were studied, one of which (labeled No. 6-2841-3) was the unirradiated, control cell. A second cell (labeled No. 6-2841-1) was irradiated with 3 MeV protons up to a fluence of  $1 \times 10^{14}$  cm<sup>2</sup>, which corresponds to a displacement damage dose<sup>2</sup> of  $D_d = 2.031 \times 10^{12}$  MeV/g. The third cell (labeled No. 6-2841-6) was first irradiated with 1 MeV electrons up to a fluence of  $1 \times 10^{16}$  cm<sup>-2</sup>, which corresponds to  $D_d$

$= 3.17 \times 10^{11}$  MeV/g, and then thermally annealed at 450 K for 2 h. Both irradiations were performed at room temperature and with the cells at open circuit.

The CL measurements were carried out on a freshly cleaved {110} face perpendicular to the plane of the  $p^+ - n$  InGaP junction. CL is excited using an electron beam in the energy ( $E_b$ ) range from 5 to 30 keV. A cryogenic charge-coupled device (CCD) (Photometrics SDS9000) was attached to an Oriel 77400 spectrograph/monochromator for spectroscopic measurements. A CTI-Cryogenics 22C/350C helium closed-circuit cryostat was used for low-temperature measurements. The TEM measurements were made in JEOL 1200EX and 2000EX transmission electron microscopes.

Figure 1 shows the CL spectra measured at 70 K with the beam centered on the  $p^+ - n$  InGaP junction. Prior to irradiation [Fig. 1(a)], three peaks are observed. The peak at 1.45 eV is attributed to free-to-bound ( $e, \text{Si}^0$ ) transitions, the others correspond to the electron–hole band-to-band transitions in GaAs and InGaP<sub>2</sub>. Figure 1(b) shows that following proton irradiation the overall CL intensity is reduced by a factor of  $\sim 300$ . Within this reduction, the InGaP-related intensity is seen to be less affected. Indeed, the GaAs/InGaP intensity ratio, which was approximately 9:2 before the irradiation, fell to 3:2 after irradiation. This change indicates that defects produced in InGaP<sub>2</sub> have a smaller effect on the car-

TABLE I. SJ  $p^+ - n$  InGaP solar cell structure.

	Material	Thickness ( $\mu\text{m}$ )	Carrier density ( $\text{cm}^{-3}$ )
Cap	$p$ GaAs	0.2	$1 \times 10^{19}$
Window	$p$ AlInP	0.025	$8 \times 10^{17}$
Emitter front surface field	$p$ InGaP	0.05	$4 \times 10^{18}$
Emitter	$p$ InGaP	0.2	$2 \times 10^{18}$
Base	$n$ InGaP	1	$\sim 1 \times 10^{16}$
Back surface field (BSF)	$n$ InGaP	0.02	$1 \times 10^{18}$
Buffer	$n$ GaAs	0.4	$2 \times 10^{18}$
Substrate	$n$ GaAs	250	$2 \times 10^{18}$

<sup>a)</sup>Electronic mail: manueljesus.romero@uca.es

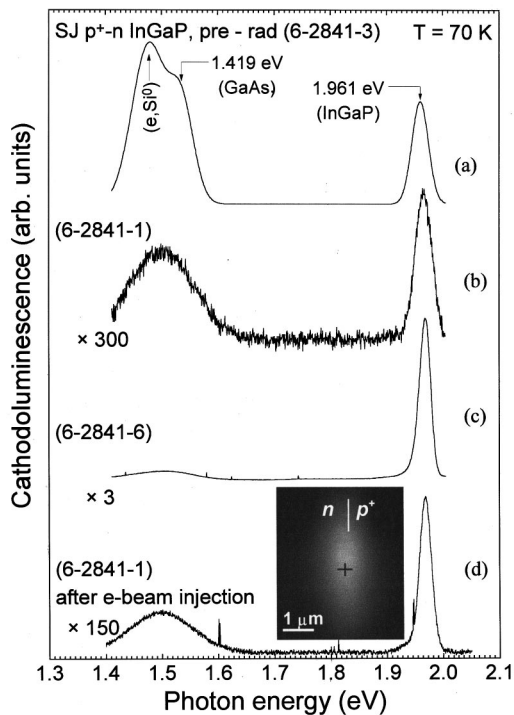


FIG. 1. CL spectra measured on  $p^+ - n$  InGaP solar cells. (a) The spectrum measured prior to irradiation. The peak centered at 1.45 eV is attributed to the free-to-bound ( $e, Si^0$ ) transition, and the peaks centered near 1.5 eV and near 2.0 eV correspond to band-to-band transitions in GaAs and InGaP<sub>2</sub>, respectively. (b) The spectrum measured after proton irradiation. The irradiation has caused an overall reduction in the CL intensity, with the bigger effect in the GaAs peak. (c) The spectrum measured after electron irradiation and subsequent thermal annealing at 450 K for 2 h. (d) CL spectrum after electron-beam injection in the  $p^+ - n$  InGaP junction ( $E_b = 20$  keV and  $I_b = 10$  nA for 1 h) of the previously proton-irradiated cell. The CL micrograph (inset) recorded after the e-beam excitation shows the spatial distribution of the luminescence recovery.

rier recombination dynamics than those induced in GaAs.

Figure 1(c) shows the CL spectrum after electron irradiation and subsequent thermal annealing. The results show that annealing increases the InGaP<sub>2</sub> band-to-band luminescence intensity to approximately 70% of the unirradiated level, whereas in GaAs the band-to-band intensity increases to only about 5% of the preirradiation level. This indicates more efficient annihilation or neutralization of radiation-induced defects in InGaP<sub>2</sub> than in GaAs.

Thermal annealing of the proton-irradiated cell was also accomplished using the electron beam as a local thermal source ( $E_b = 20$  keV and  $I_b = 10$  nA for 1 h). The inset of Fig. 1(d) shows the panchromatic CL emission measured after e-beam injection. The cross corresponds to the location of the e-beam during the thermal treatment. Since the electron beam scans the whole region, the CL has contributions from both annealed and unannealed material. The e-beam injection induced an order of magnitude increase in the InGaP<sub>2</sub> band-to-band peak intensity, indicating significant recovery of some of the radiation-induced degradation. Similar experiments on the GaAs do not produce any recovery in irradiated GaAs.

These results are in agreement with the measured photovoltaic response of irradiated InGaP<sub>2</sub> solar cells compared to radiation-induced degradation of GaAs solar cells. GaAs solar cells degrade more rapidly under irradiation than InGaP<sub>2</sub>

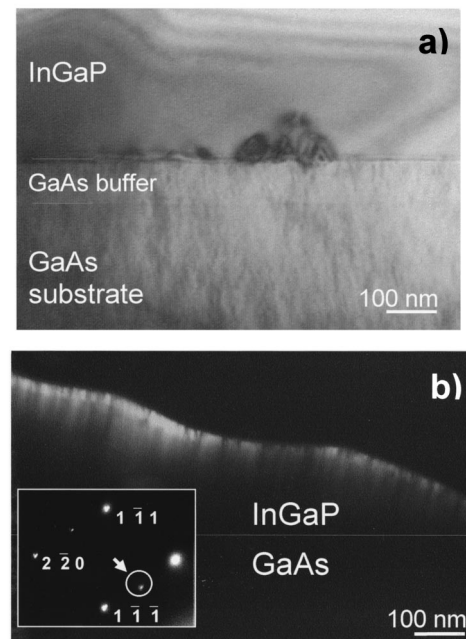


FIG. 2. (a) Bright-field BF(200) TEM micrograph showing detail of the InGaP/GaAs interface. (b) DF TEM micrograph of the InGaP epilayer taken with the superlattice spot in the SAED pattern, showing the distribution of ordered InGaP<sub>2</sub> domains. Both micrographs were taken from the unirradiated cell (6-2841-3). Subsequent irradiation removed this ordering.

cells.<sup>3,4</sup> Moreover, irradiated InGaP<sub>2</sub> solar cells show some recovery after minority-carrier injection,<sup>4,5</sup> while GaAs cells do not,<sup>6</sup> in agreement with the CL measurements reported here.

OMVPE-grown InGaP<sub>2</sub> is known for the tendency of the cations to order on the group III sublattice producing alternate In- and Ga-rich {111} planes. This sublattice ordering results in domains of ordered InGaP<sub>2</sub> within a matrix of disordered material. The ordering is a kinetic phenomenon that depends both on the orientation of the substrate<sup>7</sup> and on growth parameters such as temperature, V/III ratio,<sup>8-10</sup> and growth rate.<sup>11</sup> The cells studied here were grown by OMVPE on (001) GaAs substrates with a misorientation of 2° in the <110> direction. The growth temperature was 923 K, the V/III ratio 80, and the growth rate 0.08 μm/min. The results of Su and co-workers<sup>12,13</sup> indicate that these growth parameters lead to ordered InGaP<sub>2</sub> with a lateral domain size of around 10 nm within a disordered InGaP matrix.

TEM observations made before irradiation (cell 6-2841-3) show excellent crystal quality and indicate good lattice matching between the deposited InGaP<sub>2</sub> and the GaAs substrate [Fig. 2(a)]. The selected area electron diffraction (SAED) pattern from the InGaP<sub>2</sub> layer exhibits single variant superlattice spots. Figure 2(b) shows the corresponding dark-field (DF) TEM micrograph within one of the superlattice spots, which shows the distribution of ordered domains. The latter are extended in a direction almost parallel to the (111) plane. After irradiation, the SAED pattern from the InGaP<sub>2</sub> layer is suppressed, indicating the removal of the ordered domains. This is also evidence for a radiation-induced order-disorder transition.

The CL spectra also show indications of a radiation-induced order-disorder transition in the InGaP<sub>2</sub>. The data of Fig. 3 show that proton irradiation causes an energy shift of

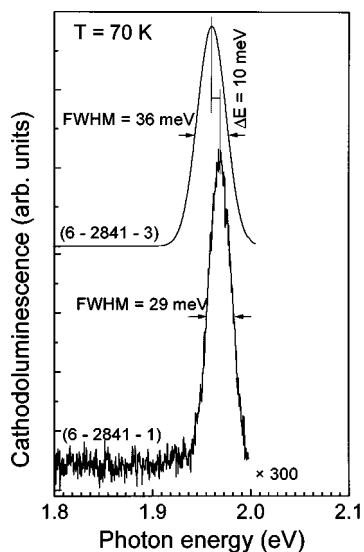


FIG. 3. Detailed analysis of the InGaP<sub>2</sub> CL peak measured before (6-2841-3) and after proton irradiation (6-2841-1). The irradiation causes a narrowing of the peak and a shift of the peak to higher energy. These effects can be explained in terms of the radiation-induced order–disorder transition.

10 meV (at  $T=70$  K) in the InGaP<sub>2</sub> luminescence peak, accompanied by a decrease in the full width at half maximum (FWHM) from 36 to 29 meV. These phenomena have also been observed after thermal annealing where ordering was predicted and experimentally observed to cause a decrease in the band-to-band transition energy and an increase of the FWHM.<sup>14,15</sup> In addition, the Varnish equation successfully fits the temperature dependence of the InGaP peak energy following irradiation, but not before (Fig. 4). Such behavior has been reported previously<sup>16,17</sup> and connected with ordering in InGaP. These CL and TEM data are all consistent with initial ordering in the InGaP<sub>2</sub> that is removed by the irradiation. Note that such an energy shift cannot be attributed to carrier removal. Indeed,  $C-V$  measurements presented in Ref. 4 show no evidence of carrier removal.

The preceding analysis illustrates how the ordering effect could be used to modulate the absorption edge in InGaP<sub>2</sub> by modifying the growth parameters at a fixed In mole fraction, without introducing any lattice mismatch. By exploiting this behavior, the spectral response of an InGaP<sub>2</sub> solar cell, and thus, the dual-junction (DJ) cell output, could possibly be optimized. Indeed, Bertness *et al.*<sup>18</sup> have suggested such an ordered–disordered (OD) heterostructure for the DJ InGaP<sub>2</sub>/GaAs technology to improve the cell efficiency. In light of this, the radiation data presented here are very important, since they indicate that if such an ordered–disordered structure were employed for a space solar cell, the beginning of life efficiency gained from the ordering phenomenon might be nullified by the effects of subsequent irradiation.

The results presented here indicate lower radiation-induced degradation of the electrical properties as well as the improved (both thermal and injection) characteristics of InGaP<sub>2</sub> compared to GaAs. These results support previous reports of the superior radiation resistance and annealing properties of InGaP<sub>2</sub> solar cells over GaAs cells. In addition, results have demonstrated ordering in as-grown InGaP<sub>2</sub> that is removed by irradiation. The radiation-induced order–

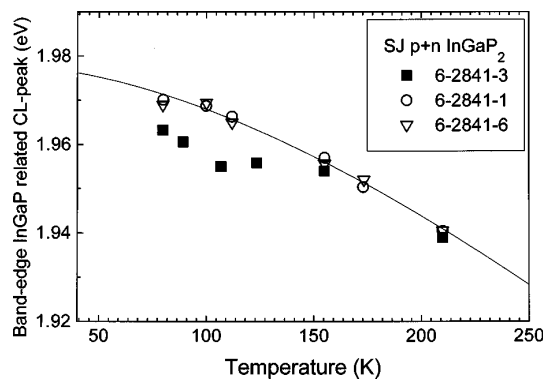


FIG. 4. Temperature dependence of the InGaP CL peak energy. The solid lines represent fits to the data to the Varnish equations. The data measured on the irradiated samples are well described by the Varnish equations, but the unirradiated data are not.

disorder transition in InGaP<sub>2</sub> caused a narrowing of the CL peak, along with a shift of the peak to higher energies. These results indicate that some measure of order-related band engineering is possible in InGaP<sub>2</sub>/GaAs DJ solar cells, but that caution must be taken in applying the technique in applications involving high-radiation environments.

This work was partially supported in Spain by the CICYT (Comisión Interministerial de Ciencia y Tecnología) under MAT94-0823-CO3-02 and by the Junta de Andalucía through Group No. TEP-0120, and in the U.S. by the Office of Naval Research.

- <sup>1</sup>T. Takamoto, E. Ikeda, and H. Kurita, *Appl. Phys. Lett.* **70**, 381 (1997).
- <sup>2</sup>The displacement damage dose ( $D_d$ ) is given by the product of the particle fluence and the calculated nonionizing energy loss (NIEL), which for 3 MeV protons is 0.0238 MeV cm<sup>2</sup>/g and for 1 MeV electrons is  $3.17 \times 10^{-5}$  MeV cm<sup>2</sup>/g in InP.
- <sup>3</sup>M. Yamaguchi, T. Okuda, S. J. Taylor, T. Takamoto, E. Ikeda, and H. Kurita, *Appl. Phys. Lett.* **70**, 1566 (1997).
- <sup>4</sup>R. J. Walters, M. A. Xapsos, H. L. Cotal, S. R. Messenger, G. P. Summers, P. R. Sharps, and M. L. Timmons, *Solid-State Electron.* **42**, 1747 (1998).
- <sup>5</sup>M. Yamaguchi, T. Okuda, and S. J. Taylor, *Appl. Phys. Lett.* **70**, 2180 (1997).
- <sup>6</sup>J. A. Bruening, Masters of Science Thesis, U.S. Naval Post-Graduate School (1993).
- <sup>7</sup>K. Sinha, A. Mascharenhas, R. G. Alonso, G. S. Horner, K. A. Bertness, S. R. Kurtz, and J. M. Olson, *Solid State Commun.* **89**, 843 (1994).
- <sup>8</sup>H. Murata, I. H. Ho, G. B. Stringfellow, and J. B. Mullin, *J. Cryst. Growth* **170**, 219 (1997).
- <sup>9</sup>Y. S. Chun, H. Murata, G. B. Stringfellow, and J. B. Mullin, *J. Cryst. Growth* **170**, 263 (1997).
- <sup>10</sup>Y. S. Chu, H. Murata, T. C. Hsu, I. H. Ho, L. C. Su, Y. Hosokawa, and G. B. Stringfellow, *J. Cryst. Growth* **79**, 6900 (1996).
- <sup>11</sup>Y. S. Chu, S. H. Lee, I. H. Ho, and G. B. Stringfellow, *J. Cryst. Growth* **174**, 585 (1997).
- <sup>12</sup>L. C. Su, I. H. Ho, and G. B. Stringfellow, *J. Appl. Phys.* **76**, 3520 (1994).
- <sup>13</sup>L. C. Su, I. H. Ho, N. Kobayashi, and G. B. Stringfellow, *J. Cryst. Growth* **145**, 140 (1994).
- <sup>14</sup>Y. Hamisch, R. Steffen, A. Forchel, and P. Rontgen, *Appl. Phys. Lett.* **62**, 3007 (1993).
- <sup>15</sup>S. H. Wei and A. Zunger, *Phys. Rev. B* **39**, 3279 (1989); S. R. Kurtz, *J. Appl. Phys.* **74**, 5326 (1994).
- <sup>16</sup>M. Kondow, S. Minagawa, Y. Inoue, T. Nishino, and Y. Hamakawa, *J. Appl. Phys.* **54**, 1760 (1989).
- <sup>17</sup>Y. Ishitani, S. Minagawa, and T. Tanaka, *J. Appl. Phys.* **75**, 5326 (1994).
- <sup>18</sup>K. A. Bertness, J. M. Olson, S. R. Kurtz, D. J. Friedman, A. E. Kibbler, and C. Kramer, Paper presented at the Electronic Materials Conference, Boulder, Colorado, June 1994.